Journal of Power Sources 214 (2012) 399–406

Contents lists available at SciVerse ScienceDirect

Journal of Power Sources

journal homepage: www.elsevier.com/locate/jpowsour

Power prediction from a battery state estimator that incorporates diffusion resistance

Shuoqin Wang [a,*], Mark Verbrugge [b], John S. Wang [a], Ping Liu [a]

[a] HRL Laboratories, LLC, Malibu 90265, CA, USA
[b] General Motors Research and Development, Warren, MI, USA

HIGHLIGHTS

- A new algorithm improves the prediction accuracy of state of power (*SOP*) of a Li-ion battery.
- It incorporates a nonlinear diffusion resistance into the formulas for the *SOP* prediction.
- The results appear very promising in testing Hitachi cells in a simulated HEV environment.
- It provides much more accurate power prediction than the original BSE.

ARTICLE INFO

Article history:
Received 5 January 2012
Received in revised form
22 April 2012
Accepted 25 April 2012
Available online 30 April 2012

Keywords:
Battery state estimator
BSE algorithm
SOC (state of charge) estimation
SOP (state of power) estimation
Equivalent circuit model

ABSTRACT

We present a new algorithm that improves the prediction accuracy of the maximum charge and discharge power capabilities, i.e. state of power (*SOP*), of a battery state estimator (BSE) using an equivalent-circuit representation of a battery. For short time (high frequency) operation, lithium ion traction batteries are often dominated by ohmic and interfacial kinetic resistance, and conventional equivalent circuits employing resistors and capacitors (RC circuits) work well to characterize the system. However, for longer times, diffusion resistance becomes important and conventional BSEs based on RC elements fail to provide useful power predictions. In order to take into account diffusion in the *SOP* prediction, we propose to incorporate a nonlinear resistance into the power prediction formulas that are otherwise based on an RC circuit formulation; The diffusion effect is addressed with this nonlinear resistance whose value is proportional to the square root of time. The new approach is implemented in a vehicle-simulation environment (a hardware-in-the-loop setup) to predict the *SOP* of a lithium-ion battery. Simulation results demonstrate that this revised estimator provides much more accurate power prediction without compromising the regression performance of the original BSE.

1. Introduction

In many battery-powered systems such as electric vehicles (EV) and hybrid electric vehicles (HEV), the efficiency of traction batteries can be greatly enhanced by intelligent management of the electrochemical energy storage system [1]. These applications require a battery state estimator (BSE) to ensure accurate and timely estimation of the state of charge (*SOC*), the charge and the discharge power capabilities (*SOP*), and the state of health (*SOH*). In this work, we focus on the *SOP* predictions of HEV lithium ion batteries.

Various battery models have been studied within the framework of a BSE [2–17]. A physics-based electrochemical model may be able to capture the temporally evolved and spatially distributed behavior of the essential states of a battery [2,3,16,17]. Such analyses are built upon fundamental laws of transport, kinetics and thermodynamics, and require inputs of many physical parameters. Because of their complexity, longer simulation times are needed, and there is no assurance of convergence in terms of state estimation. Thus, while these more complex models are suitable for battery design and analysis, they have not been used in commercial BSEs. Due to limited memory storage and computing speed of embedded controllers employed in many applications and the need for fast regression in terms of parameter extraction, a (zero dimensional) lumped parameter approach based on an equivalent circuit model has been found to be most practical for BSE formulation. A circuit employing

* Corresponding author. Tel.: +1 310 317 5183; fax: +1 310 317 5840.
E-mail address: swang@hrl.com (S. Wang).

0378-7753/$ – see front matter © 2012 Elsevier B.V. All rights reserved.
doi:10.1016/j.jpowsour.2012.04.070

a resistor in series with a circuit element comprising a parallel resistor and capacitor (an R-RC circuit, see Fig. 1) has been employed successfully for embedded controllers [6,14,15,18–24]. It should be noted that this approach is fundamentally correct only when the battery is exposed to small as well as high frequency signal perturbations around equilibrium; in this case, the parameter value can be traced back to those appearing in the more complex physical models mentioned above. Highly non-equilibrium behavior of the battery is difficult to address with a simple R-RC circuit. For such behavior, more physical effects need to be included along with a more detailed model, at the expense of the simplicity and robustness [3–5].

Recently we have published an adaptive, multi-parameter direct-differential (DD) algorithm based on the direct solution of the differential equations that govern an equivalent-circuit representation of the battery [24]. The short-term *SOP* projection was shown to agree well with the experimental values, but the long-term *SOP* projections deviated from measurements. The deviation could exceed 30% for the 10-s *SOP* projections. A battery's long-term power output is subject to mass-transfer limitations (diffusion resistance), be it due to salt diffusion within the separator phase or lithium diffusion within the solid state. The well-known Warburg impedance can represent diffusion resistance in many cases in the frequency domain [25]. However, it is not straightforward to incorporate Warburg impedance in an equivalent circuit model analytically because it is frequency-dependent and therefore a nonlinear device. The Warburg impedance can also be approximated with many pairs of parallel RC circuits [26]. Therefore two or three RC-circuit models have been studied, in which one RC combination is used to represent electron-transfer kinetics, and another one or two RC combinations approximate diffusion contributions. However, our experience is that multiple RC models do not work sufficiently well for long-term *SOP*. Moreover, use of multiple RC combinations compromises the regression stability of a BSE when compared to a simple R-RC circuit.

We propose in this paper to address diffusion resistance with a term $R_{diffusion}$ that is linearly proportional to the square root of time and is dependent on the open circuit voltage. That is, in order to make up for the omission of diffusion from the parameter identification scheme used to characterize the state of the battery, we add in the time-dependent diffusion correction $R_{diffusion}$ to the power projection algorithm, thereby approximating the impact of diffusion. We develop the formula of $R_{diffusion}$ based on its practicality in terms of improving the *SOP*. Because $R_{diffusion}$ is absent in parameter regression of the circuit model, the utility and simplicity of the R-RC regression is kept intact. Last, we show that hundreds of randomized power tests demonstrate the enhancement of the *SOP* prediction employing $R_{diffusion}$.

The following sections are organized as follows. Section 2 discusses the diffusion issue in the context of the *SOP* prediction. Section 3 details the R-RC circuit model incorporating the diffusion resistance $R_{diffusion}$. The schematic of the model, the regression scheme, the expression for $R_{diffusion}$, and the analytical equations of power outputs are provided there. Section 4 describes the experimental setup including essential hardware and software elements. Section 5 discusses experimental results demonstrating the *SOP* improvement with the inclusion of the diffusion resistance $R_{diffusion}$. Finally, a summary and an overview of open questions are provided in Section 6.

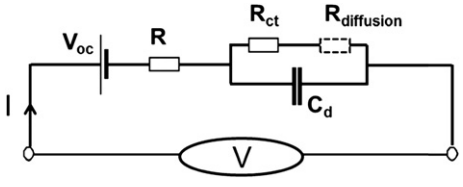

Fig. 1. Equivalent circuit model of the battery system. $R_{diffusion}$ is only used in power calculation but is absent in the circuit regression. Positive current denotes the charge process. In the absence of $R_{diffusion}$, the schematic reflects the R-RC circuit mentioned in the text.

2. *SOP* deviation and the diffusion issue

Before we introduce the *SOP* deviation and its diffusion issue, we need to briefly discuss how we deduce the *SOP* and evaluate its accuracy. In an R-RC circuit model (Fig. 1), the algorithm regresses recursively the model parameters such as the open circuit voltage (V_{oc}), the high-frequency resistance (R), the charge-transfer resistance (R_{ct}) and double-layer capacitance (C_d), based on inputs including the battery current and voltage. The *SOP*, which is the maximum charge and discharge power capabilities of a cell, can then be calculated in real time using the regressed parameters of RC elements and V_{oc} [18]. In order to evaluate the algorithm on the *SOP* prediction, a battery's maximum power capabilities are measured after each driving process. Such a power test is essentially an analog of a potential-step excitation, in which the maximum discharge power is measured by setting the battery voltage to its lowermost limit and recording the discharge current against time. The maximum charge power is similarly measured by setting the battery voltage to the uppermost limit and recording the charge currents against time. More information about the power tests is provided in Section 4.

Fig. 2 highlights the *SOP* deviation by comparing the calculated powers with the measured values acquired in a typical power test,

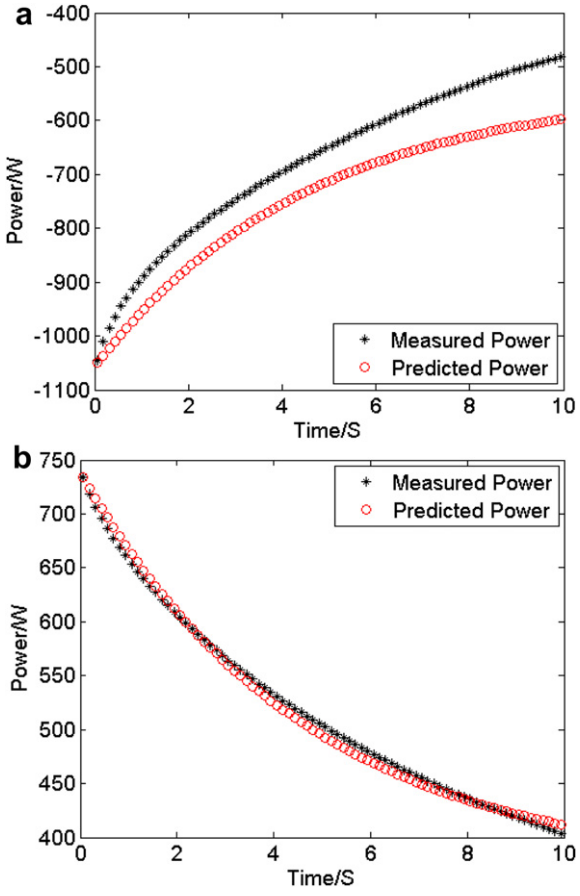

Fig. 2. Measured power and predicted powers of a Li-ion cell verse time. The predicted powers were calculated based on the R-RC circuit model [24]. (a) Corresponds to a discharge power test and (b) to a charge power test.

with Fig. 2(a) for the discharge power test and 2(b) for the charge power test. The predicted values are close to the measured values at short times but deviate from the measured values for longer times. It may be explained that in the beginning, the power is mainly determined by electron-transfer kinetics; therefore the faradaic impedance can be approximated with a linear charge-transfer resistance [25]. In the longer term, the battery current is likely influenced by diffusion resistance. Fig. 2 also demonstrates that the *SOP* deviation is more severe for discharge than charge, indicating the diffusion effect may be more dominant in discharge cases, which is consistent with the experiment results published in the Ref. [24].

Diffusion resistance is revealed more clearly in Fig. 3, which is based on several *SOP* measurements at different values of V_{oc}. We choose $It^{1/2}$ for the ordinate of the figure because the diffusion-limited current may be approximated by the Cottrell equation [25] and therefore the diffusion region would be manifest as a plateau in the figure. As it is shown in Fig. 3(a), the discharge currents appear to transition from kinetic control initially to diffusion control (plateaus) in the longer term. We can also deduce from the figure that as the V_{oc} increases, diffusion control takes place earlier. Fig. 3(b), which corresponds to the charge power tests, shows no obvious plateaus during the 10-s period, verifying that the diffusion effect is smaller during charge, and therefore the R-RC circuit model can predict charge power with small error without addressing diffusion for the conditions investigated [24].

Electrochemical impedance spectroscopy (EIS) analysis was also conducted on the cell as shown in Fig. 4. The battery impedance $Z(\omega) = Z'(\omega) - iZ''(\omega)$ was measured from 0.01 Hz to 10 Hz. The measurements were performed at four different values of V_{oc}. Two different regimes are depicted in Fig. 3: the semicircles capture ohmic and interfacial kinetics losses at higher frequencies, and diffusion (e.g., Warburg) impedance is seen at lower frequencies. We can roughly estimate that for frequencies lower than 3 Hz, the diffusion starts to impact the kinetic behavior. We may therefore expect that in the time-domain, for power predictions of durations longer than a third of a second, diffusion resistance will play an important role. It should be noted that EIS is normally conducted with small-signal (current or voltage) perturbations and therefore the cell is around equilibrium during the experiment, which may be somewhat different from the maximum power test experiment, wherein the cell is driven far away from equilibrium.

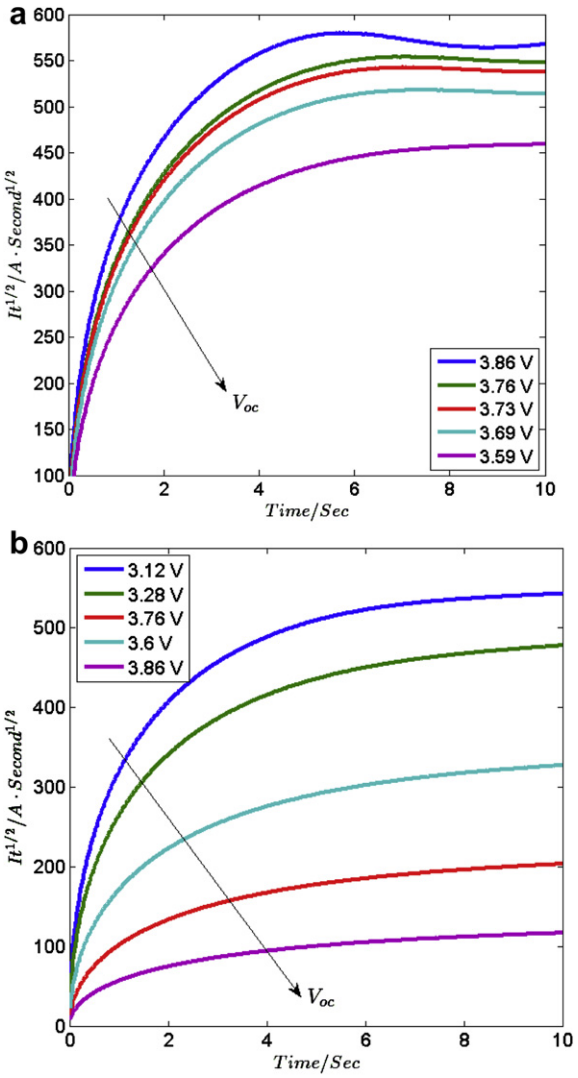

Fig. 3. The plots of $It^{1/2}$ *vs. t. I* is the measured current. Each curve results from a power test with the battery is set at its corresponding V_{oc}. (a) Corresponds to the discharge cases and (b) to the charge cases.

3. Theory of the R-RC circuit model including diffusion resistance

Fig. 1 illustrates the one RC circuit model, based on which the regression algorithm (BSE) and the power equations are derived. As we mentioned in the first section, the diffusion resistance $R_{\text{diffusion}}$ is only used in the power calculation, but not in the parameter regression. The governing equation for the regression is derived as following with the application of Kirchhoff's circuit laws

$$V = (R + R_{ct})\, I + RR_{ct}C_d\frac{dI}{dt} - R_{ct}C_d\frac{dV}{dt} + V_{oc} \tag{1}$$

In Eq. (1), V and I are measured inputs (their time derivatives being derived directly from measurements) and R, R_{ct}, C_d, and V_{oc} are model parameters needed to be regressed at each time step. Therefore, the formalism corresponds to a parameter identification

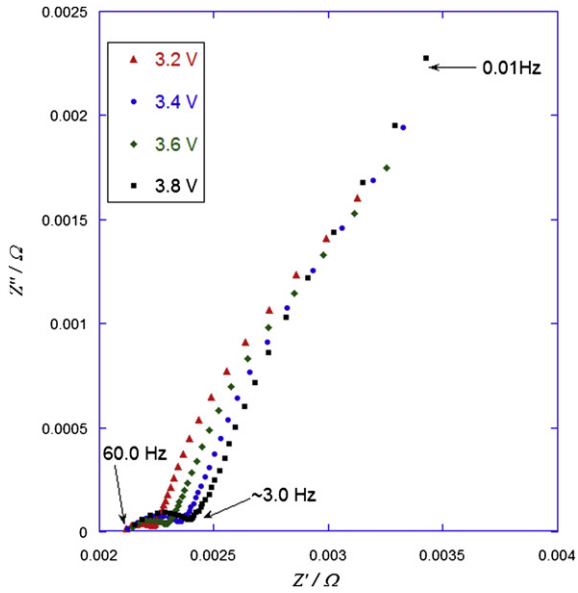

Fig. 4. Impedance spectra of a Li-ion cell measured at four different open circuit potential V_{oc}. Z′ and Z″ are the real and imaginary impedance response of the battery. The frequencies were swept from 0.01 Hz to 60 Hz with 10 logarithmically interval.

problem [27]. The parameters are regressed by applying the measured values of the current I and voltage V of the battery in real time. The derivatives of the current and voltage over time are approximated with difference equations: $dI/dt = (I(t) - I(t-\Delta t))/\Delta t$ and $dV/dt = (V(t) - V(t-\Delta t))/\Delta t$. The weighted-recursive-least-square (WRLS) method is applied to regress the model parameters [27,28]. The method is briefly described as follows. Consider a linear dynamic model with input variables $\{x_l(t), l = 1,2,\ldots,L\}$ and output variable $y(t)$ and assume these variables are sampled at discrete times $\{t_j, j = 1,2,3,\ldots,N\}$ and further assume that the sampled values can be related through the linear equation

$$y(t_j) = \sum_{l=1}^{L} m_l x_l(t_j) \tag{2}$$

where $\{m_l, l = 1,2,\ldots,L\}$ are the l parameters to be identified. In the WRLS method, the parameters are determined by minimizing the sum of the weighted square of the error terms

$$\varepsilon = \sum_{l=1}^{L} \varepsilon_l = \sum_{l=1}^{L}\sum_{j=1}^{N} \lambda_l^{N-j}\left[y(t_j) - \sum_{l=1}^{L} m_l x_l(t_j)\right]^2, \tag{3}$$

where $\{\lambda_l, l = 1,2...L\}$ are the L exponential forgetting factors for time-weighting data. A larger weight factor λ_l gives rise to a larger error term, ε, and thus more influence with regard to evaluating the parameter m_l. The approach we employ allows for multiple forgetting factors and is described in more detail in Ref. [18]. The following assignments are made:

$$\begin{array}{l} y(t) = V(t) \\ x_1 \text{ to } x_4 = I, \quad (dI/dt), \quad (dV/dt), \quad 1 \\ m_1 \text{ to } m_4 = R + R_{ct}, \quad RR_{ct}C_d, \quad R_{ct}C_d, \quad V_{oc} \end{array} \tag{4}$$

The four m_l parameters are updated at each time step, based on which model parameters (e.g.,R, R_{ct}, C_d, V_{oc}) are being regressed.

The formula for the battery *SOP* prediction at the real time has been derived as [18]

$$P\left(t\right) = IV_{\text{Limit}} = V_{\text{Limit}}\frac{V_{\text{Limit}} - V_{oc}}{R + R_{ct}} + V_{\text{Limit}}\left(\frac{V_{\text{Limit}} - V + IR}{R} - \frac{V_{\text{Limit}} - V_{oc}}{R + R_{ct}}\right)\exp\left(-\frac{R + R_{ct}}{RR_{ct}C_d}t\right),$$

where I and V are the measured current and voltage at the start of the constant -voltage event. The maximum discharge power capability is calculated with V_{Limit} set to the mimimum battery voltage; and the maximum charge power capability is calculated with V_{Limit} set to the maximum battery voltage.

In order to take into account of the diffusion effect which is not included in the above equation, we add on the charge-transfer resistance R_{ct} with a diffusion resistance, as shown in Fig. 1. We define the diffusion resistance as

$$R_{\text{diffusion}} = A\sqrt{\frac{t}{\tau}} \tag{5}$$

with

$$\tau = \left|e^{B} - e^{V_{oc}}\right| \tag{6}$$

τ is used in the equation of $R_{\text{diffusion}}$ to approximate the time upon which the battery power evolves from control by interfacial resistance to control by diffusion [25]. As illustrated in Fig. 3, this transition time is a function of V_{oc}. In the above two equations, A and B are two empirical parameters. A can be used to adjust the importance of diffusion resistance relative to interfacial and ohmic resistance. B is used to adjust the dependence of τ on V_{oc}. Moreover, in order to accommodate the possibility of different electrode kinetics processes for charge and discharge [29,30], we use two sets of A and B values, A_c and B_c or A_d and B_d, (subscript c for charge and d for discharge) for charge and discharge respectively. For example, we may choose a larger A for $R_{\text{diffusion}}$ in the discharge power calculation, since diffusion is more prominent in discharge power tests than in charge power tests. We will discuss how to determine A and B values in Section 4.

By incorporating the $R_{\text{diffusion}}$, the analytical equations for *SOP* predictions are formulated in following equations (Eqs. (7)–(10)). The charge power capability is obtained when the battery voltage is fixed to its maximum value:

$$P_{\text{charge}}\left(t\right) = I_{\text{charge}}V_{\max} = V_{\max}\frac{V_{\max} - V_{oc}}{R + R_{ct\_c}} + V_{\max}\left(\frac{V_{\max} - V + IR}{R} - \frac{V_{\max} - V_{oc}}{R + R_{ct\_c}}\right)\exp\left(-\frac{R + R_{ct\_c}}{RR_{ct\_c}C_d}t\right) \tag{7}$$

where

$$R_{ct\_c} = R_{ct} + R_{\text{diffusion\_c}} = R_{ct} + A_c\sqrt{\frac{t}{\left|e^{B_c} - e^{V_{oc}}\right|}} \tag{8}$$

The discharge power capability is obtained when the battery voltage is fixed to its minimum value:

$$P_{\text{discharge}}\left(t\right) = I_{\text{discharge}}V_{\min} = V_{\min}\frac{V_{\min} - V_{oc}}{R + R_{ct\_d}} + V_{\min}\left(\frac{V_{\min} - V + IR}{R} - \frac{V_{\min} - V_{oc}}{R + R_{ct\_d}}\right)\exp\left(-\frac{R + R_{ct\_d}}{RR_{ct\_d}C_d}t\right) \tag{9}$$

where

$$R_{ct\_d} = R_{ct} + R_{\text{diffusion\_d}} = R_{ct} + A_d\sqrt{\frac{t}{\left|e^{B_d} - e^{V_{oc}}\right|}} \tag{10}$$

It should be noted that in order to avoid the possible zero value in the denominators of both Eqs. (8) and (10), the value of B should be chosen outside the range of the possible V_{oc} values; Or in the denominators of above two equations a very small and positive number can be added outside the absolute value.

4. Experimental setup

In order to evaluate the algorithm in *SOP* prediction under simulated driving conditions, the algorithm was implemented and integrated with a hardware-in-the-loop (HIL) system [31]. The battery used in the experiments was a single-cell lithium ion battery (Hitachi Automotive Products, model # A23-06H04-G00) which has a nominal capacity of 5.6 Ah and a voltage range of 2.9–4.0 V. All tests were conducted at room temperature.

The architecture of the HIL consists of three components: the electrochemical cell (EC) interface, the vehicle model, and the HIL controller. The communications between these three modules are realized with TCP/IP protocols. The EC interface acts as an environmental interface to the electrochemical cell under test, and its main facilities include a single-channel tester (BT2000, Arbin Instruments) that can provide up to 5 kW at potentials between 0.6 and 5 V ± 1 mV and current ranges up to 1 kA ± 10 mA. The vehicle model is the Hybrid Powertrain Simulation Program

(HPSP) provided by GM. HPSP provides electric-power requirements based on specific driving profiles. The HIL controller serves as the command center in safeguarding the process. For example, in a cycling process, as a power request is received from HPSP, the HIL controller analyzes the request and, if valid, sends the request to the EC interface, receives the I-V-T response from the interface, iterates through the algorithm with the I-V-T data, and provides feedback to the HPSP for its preparation of its next power request. Concurrently, the HIL controller must continuously monitor the system to ensure operation within specified limits so as to avoid cell abuse. The algorithm is written in C++ and is embedded within the controller. Execution of the algorithm for regressing the model parameters in real-time requires initializing values for certain parameters and setting their allowed bounds. This is necessary since in a real vehicle environment, noise (e.g., due to electro-magnetic interference) may lead the regression to spurious predictions. The initial values, allowable boundaries, and forgetting factor λ of each parameter used in the experiments are tabulated in Table 1. As shown in the table, the upper and lower boundaries for the parameter values are set to be ten times larger or smaller than their initial values. In the present work, all λ_l were set to $\lambda = 0.999$ for simplicity. The initial value of the parameter V_{oc} was set to be the measured voltage at the start of the regression. Based on initial values, boundary conditions, forgetting factors of the parameters and the updated variables *I, V* of the battery, the algorithm regresses the model parameters recursively. The procedures for power tests presented in this paper are summarized as follows:

- An initial *SOC* value was randomly selected ranging from 30 to 75%. (The corresponding open circuit potential V_{oc} was obtained via a look-up table containing V_{oc} and associated *SOC* values [24].) The battery was charged or discharged with a current rate of C/6 until reaching the selected value of V_{oc}, where it was allowed to rest for 60 min.
- The cycling profile was randomly selected from anyone of the four driving profiles as shown in Fig. 5. The cycling process lasted at least 10 min, during which the battery voltage and current were sampled every 100 ms.
- The cycling process was stopped at a randomly selected time, and a choice of test (either max charge power test, or max discharge power test) was randomly made. The charge or discharge power tests were performed by commanding on the battery the maximum voltage of 4.0 V or minimum voltage of 2.9 V, and tracing the current response as a function of time. The measured charge or discharge power capability as the function of time was determined by multiplying the current trace by the maximum or minimum voltage, respectively.

Table 1
Initial (seed) values and bounds for the parameters used for the regression of the simplified version of the DD algorithm. The forgetting factor for each parameter was set to 0.999 in this work.

Quantity, units	Initial value	Boundary values [min, max]
R, mohm	4	[0.4, 40]
R_{ct}, mohm	2.5	[0.25, 25]
C_d, F	4000	[400, 40,000]
V_{oc}, V	Measured voltage-value at $t = 0$	[2.7, 4.1]
w (weighting factor)	0.995	
Ah_{nominal}, Ahour	5.6	
$V_{\min}$(Power), V	2.9	
$V_{\max}$(Power), V	4.0	

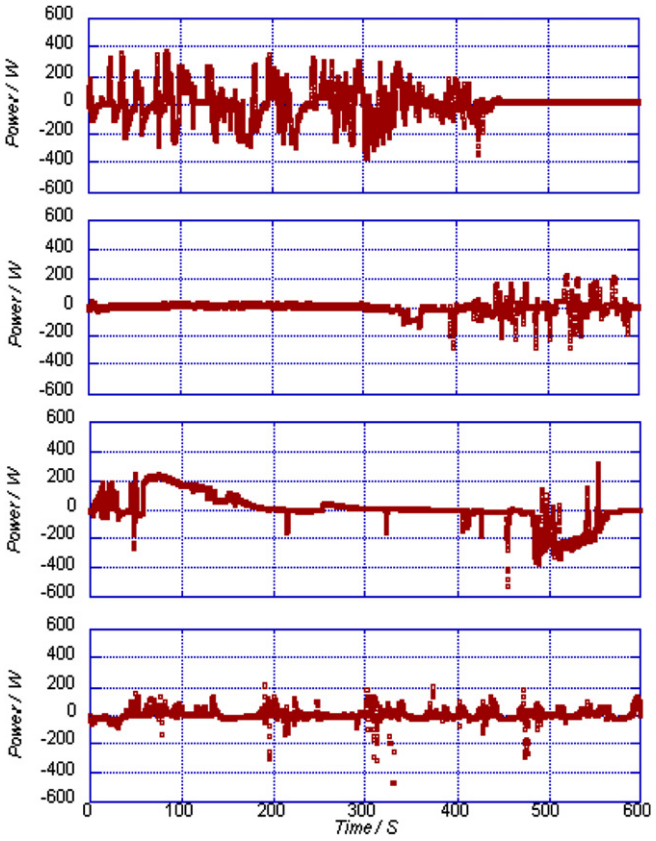

Fig. 5. Four different driving profiles that were randomly selected for the cycling process of a Li-ion battery cell. The driving profiles were acquired from testing vehicles driven at four different places and the power data have been scaled down to the cell level. Only 600 s of profiles were drawn here for demonstration.

5. Experimental results and discussion

Fig. 6 highlights a typical parameter-regression result from the simplified algorithm during the cell cycling process. As shown in the figure, the high-frequency resistance R remains almost the same throughout the driving process, consistent with a constant number of charge carriers in the electrolyte phases, and little change in the solid phase electronic resistance in the lithium ion battery. All parameters were regressed within their preset boundary values, indicative of algorithm stability.

The empirical values of A and B to be used in the $R_{\text{diffusion}}$ calculation were acquired by fitting the measured discharge and charge powers vs. time curves with the Eqs. (7) and (9) respectively. Since inside Eqs. (7) or (9), all the parameter values are known from the real-time regression except $R_{\text{diffusion}}$, we are able to isolate optimal values for A and B in this manner. The Levenberg–Marquardt method was applied for this nonlinear fit [32]. Fig. 7(a) and (b) demonstrate the curve-fitting results on the measured discharge and charge powers respectively. For comparison, the calculated powers without considering $R_{\text{diffusion}}$ (i.e., $R_{\text{diffusion}} = 0$ in Eqs. (7) and (9)) are also plotted. The optimized A and B values for representing charge power projections were near 0.0002 Ohm and 3.8 V, respectively. For the discharge power projections, the corresponding values were 0.002 Ohm and 4.0 V, respectively. The optimized A for the discharge power test is ten times larger than the A for the charge-power test, consistent with the earlier observation that the diffusion effect is more prominent in discharge power case than in the charge-power case.

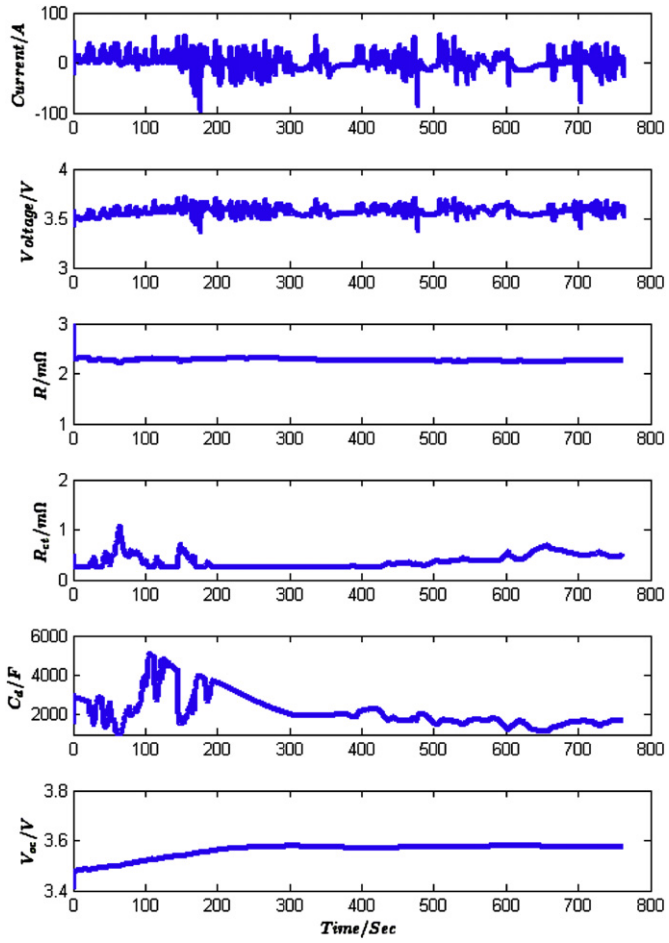

Fig. 6. The regressed parameters R, R_{ct}, C_d, V_{oc} as the function of time during the cycling process with driving profile of I-t and V-t plotted at the top of the figure.

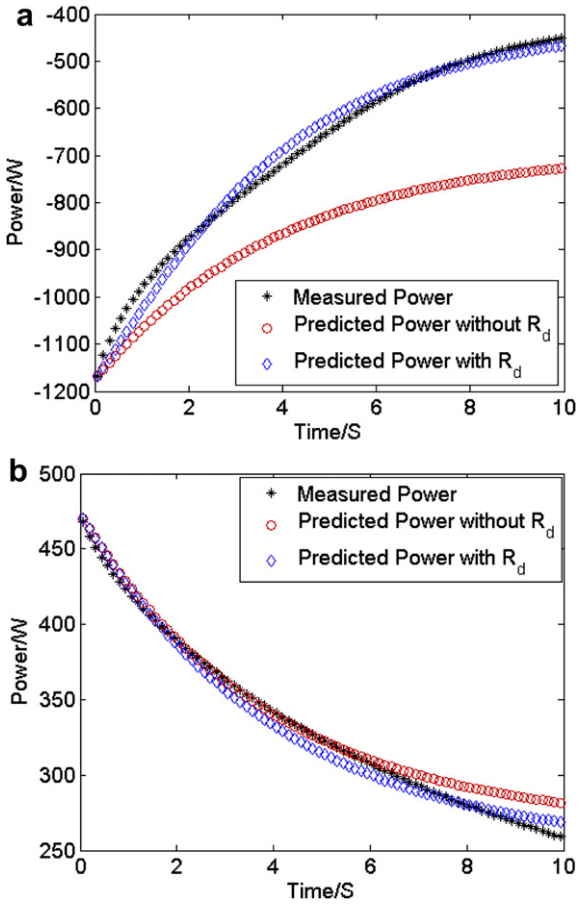

Fig. 7. The comparison between the measured power as the function of time and the predicted power projections in the maximum discharge power test event (Fig.(a)) and in the maximum charge power test event (Fig. (b)), respectively. In these two figures, the predicted powers without $R_{\text{diffusion}}$ are calculated with $R_{\text{diffusion}} = 0$ in Eqs. (7)–(9). The predicted powers with $R_{\text{diffusion}}$ are acquired by curve-fitting the measured powers with Eqs. (7)–(9).

A significant concern for this technique is stability of the A and B values relative to different circumstances (e.g., different drive events). We performed dozens of random power tests (random initial SOCs, testing durations, and test schedules) and the optimized values of A and B were acquired as shown in Fig. 8. In discharge cases, the best values of A have a mean of 0.002 with ~30% standard deviation, and B a mean of 4.0 with ~5% deviation; in charge cases, the best values of A have a mean of 0.0002 with ~10% deviation, and B a mean of 3.9 with ~10% deviation. We conclude from the plots that the values A and B were quite stable around the above mentioned optimized values. However, the optimized values of A and B may change due to aging of a battery; the above procedures identify A and B values that can be used to update A and B adaptively.

Finally we conducted more than three hundred random power tests during a three-month period with the fixed A and B values in the algorithm, and summarized results in Fig. 9. All of the tests were performed with the battery at the room temperature. Each data point in the figure corresponds to a random test, and negative (positive) powers refer to the discharge (charge) power tests. We compare the measured powers with the predicted powers at three given times; i.e., at 0 s (instantaneous power projection), 2 s (short-term), and 10 s (long-term). Fig. 9(a) and (b) provide the comparison between experiment and the SOP algorithm without $R_{\text{diffusion}}$. The instantaneous SOP prediction for both charge and discharge power tests is always accurate, indicating the consistency in regressing the high frequency resistance R. The charge-power projections are quite accurate for the SOP at short times but are slightly larger than the measured values at long times. The discharge-power projections are larger than those measured at both short and the long times. The deviations tend to grow as the power magnitude increases. The deviation can reach 20% and 50% for short and long times, respectively. Fig. 9(c) and (d) provide the comparison between experiment and the SOP algorithm with $R_{\text{diffusion}}$. The SOP prediction for the discharge cases improves significantly, with the deviation within 2%; and modest improvement is seen for the charge cases, with the deviation within 10%.

6. Summary and open questions

We have demonstrated a simple and practical technique to improve the SOP prediction significantly without compromising the simple and stable regression behavior of conventional algorithms. Specifically, we have proposed and implemented a technique to incorporate diffusion resistance in formulating the power prediction equation. The technique may be useful in supplementing other RC circuits used for BSEs for the purposes of power prediction.

Several open questions remain. First, we have not addressed the influence of temperature. If the empirical parameters used in calculating the diffusion resistance $R_{\text{diffusion}}$ are sensitive to temperature, then we may need to build a look-up table in order for

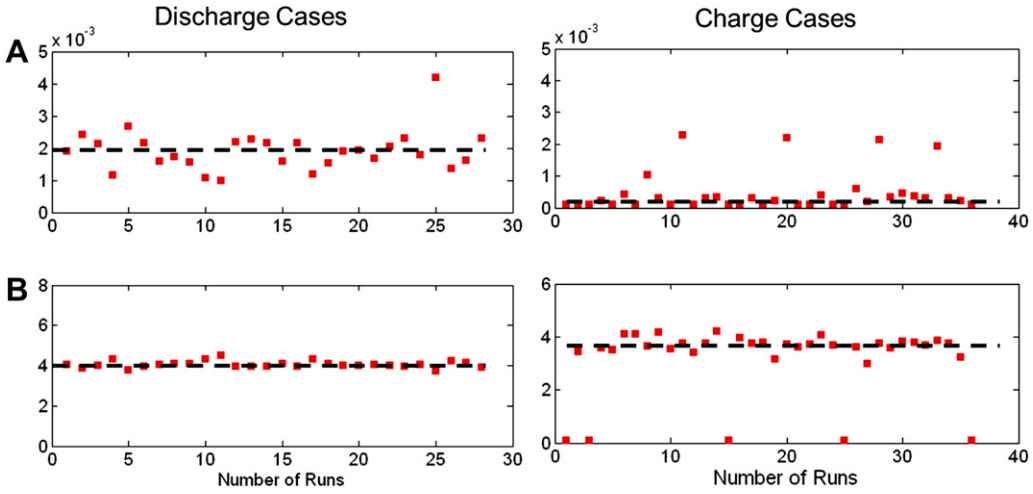

Fig. 8. The best A and B values resulted from the curve-fits of power data measured from dozens of random power tests. For discharge $A \approx 0.002$ and $B \approx 4.0$. For charge, $A \approx 0.0002$ and $B \approx 3.8$. These values marked as dash lines in respective cases.

the algorithm to select the best parameter values for different temperatures. Second, the derivation of the power equation is based on the assumption that $R_{\text{diffusion}}$ is a conventional resistance that can be simply added to that of the charge-transfer resistance to modify the power projection equation. While this approach has been shown to work well in this study, the generality of the approach can be questioned. A more rigorous formulation can be derived, but that is beyond the scope of this work. Third, diffusion is not considered in the R-RC regression. It may be that other batteries, particularly those for pure electric vehicle applications that have thicker electrodes and larger particles, will encounter greater diffusion resistance. In that case, we may need to include in the regression a nonlinear circuit element that mimics diffusion processes.

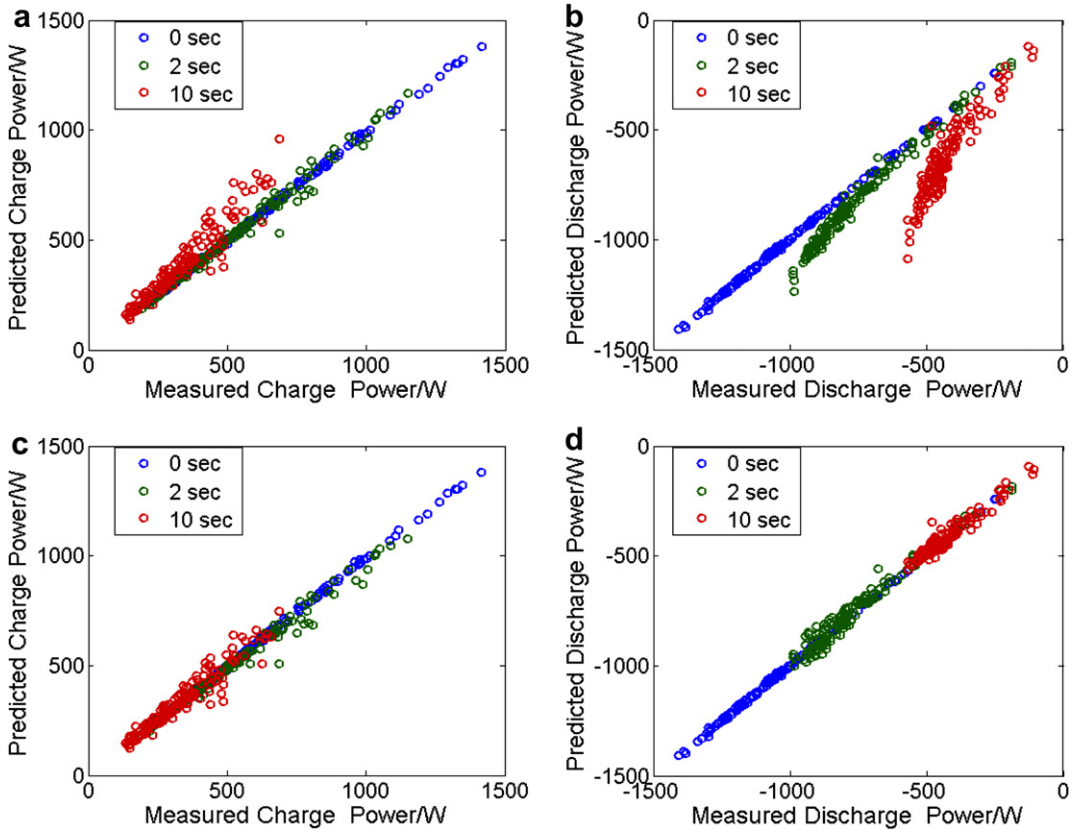

Fig. 9. Summary of random tests for the 0, 2, and 10 s *SOP* tests. Each point corresponds to one test. The *SOP* power projections correspond to the ordinate, and the abscissa values reflect measurements. Figures (a) and (b) are plotted based on the power calculation without $R_{\text{diffusion}}$, and (c) and (d) are based on the calculation with $R_{\text{diffusion}}$.

Acknowledgments

We appreciate the help of Souren Soukiezian of HRL in setting up the experiment and measuring the initial battery capacities, and Brian Koch of GM Product Development in providing relevant information.

References

[1] M. Verbrugge, Adaptive Characterization and Modeling of Electrochemical Energy Storage Devices for Hybrid Electric Vehicle Applications chap. 8, in: M. Schelsinger (Ed.), Modern Aspects of Electrochemistry No. 43: Modeling and Numerical Simulations I, first ed. Springer, 2009.
[2] M. Doyle, T.F. Fuller, J. Newman, J. Electrochem. Soc. 140 (1993) 1526.
[3] J. Newman, W. Tiedemann, AIChE J. 21 (1975) 25.
[4] A.P. Schmidt, M. Bitzer, Á.W. Imre, L. Guzzella, J. Power Sources 195 (2010) 5071.
[5] K.A. Smith, IEEE 30 (2010) 18.
[6] N.A. Chaturvedi, R. Klein, J. Christensen, J. Ahmed, A. Kojic, IEEE 30 (2010) 49.
[7] Y. Hu, S. Yurkovich, Y. Guezennec, R. Bornatico, American Control Conference (2008) p. 318.
[8] P.L. Moss, G. Au, E.J. Plichta, J.P. Zheng, J. Electrochem. Soc. 155 (2008) A986.
[9] P. Pisu, G. Rizzoni (Eds.), Vehicle Power and Propulsion, 2005 IEEE Conference (2005) p. 8.
[10] G.L. Plett, J. Power Sources 134 (2004) 252.
[11] S. Santhanagopalan, Q.Z. Guo, P. Ramadass, R.E. White, J. Power Sources 156 (2006) 620.
[12] S. Santhanagopalan, R.E. White, J. Power Sources 161 (2006) 1346.
[13] S. Santhanagopalan, R.E. White, Int. J. Energy Res. 34 (2010) 152.
[14] Y. He, W. Liu, B.J. Koch, J. Power Sources 195 (2010) 2969.
[15] H. Asai, H. Ashizawa, D. Yumoto, H. Nakamura, Y. Ochi, SAE Trans. 114 (2005) 205.
[16] W. van Schalkwijk, B. Scrosati, Adv. Lithium-Ion Batteries (2002).
[17] L. Cai, R.E. White, J. Power Sources 196 (2011) 5985.
[18] M. Verbrugge, J. Appl. Electrochem. 37 (2007) 605.
[19] M. Verbrugge, E. Tate, J. Power Sources 126 (2004) 236.
[20] S. Pillar, M. Perrin, A. Jossen, J. Power Sources 96 (2001) 113.
[21] M. Verbrugge, D. Frisch, B. Koch, J. Electrochem. Soc. 152 (2005) A333.
[22] M. Verbrugge, B. Koch, J. Electrochem. Soc. 153 (2006) A187.
[23] M.W. Verbrugge, R.S. Conell, J. Electrochem. Soc. 150 (2003) A1153.
[24] S. Wang, M. Verbrugge, J. Wang, P. Liu, J. Power Sources 196 (2011) 8735.
[25] Allen J. Bard, Larry R. Faulkner, Electrochemical Methods, John Wiley & Sons, Inc, 2001.
[26] N.A. Sekushin, Russ. J. Electrochem. 45 (2009) 828.
[27] L. Ljung, T. Sodedrstrom, Theory and Practice of Recursive Identification, MIT press, Cambridge.
[28] A. Vahidi, A. Stefanopoulou, H. Peng, Vehicle Syst. Dyn. 43 (2005) 31.
[29] M.W. Verbrugge, R.S. Conell, J. Electrochem. Soc. 149 (2002) A45.
[30] M.W. Verbrugge, R.Y. Ying, J. Electrochem. Soc. 154 (2007) A949.
[31] C. Massey, A. Bekaryan, M. Verbrugge, T. Weber, D. Frisch, L. Turner, A. Perulian, P. Liu, SAE Commercial Vehicle Engineering Conference, SAE International, Warrendale, PA, 2005.
[32] G.A.F. Seber, C.J. Wild, Nonlinear Regression, Wiley-Interscience, Hoboken, NJ, 2003.